International Journal of Thermophysics, Vol. 21, No. 5, 2000

Molar Heat Capacity C_v, Vapor Pressure, and (p, ρ, T) Measurements from 92 to 350 K at Pressures to 35 MPa and a New Equation of State for Chlorotrifluoromethane (R13)

J. W. Magee,[1,2] S. L. Outcalt,[1] and J. F. Ely[1,3]

Received May 22, 2000

Measurements of the molar heat capacity at constant volume C_v for chlorotrifluoromethane (R13) were conducted using an adiabatic method. Temperatures ranged from 95 to 338 K, and pressures were as high as 35 MPa. Measurements of vapor pressure were made using a static technique from 250 to 302 K. Measurements of (p, ρ, T) properties were conducted using an isochoric method; comprehensive measurements were conducted at 15 densities which varied from dilute vapor to highly compressed liquid, at temperatures from 92 to 350 K. The R13 samples were obtained from the same sample bottle whose mole fraction purity was measured at 0.9995. A test equation of state including ancillary equations was derived using the new vapor pressures and (p, ρ, T) data in addition to similar published data. The equation of state is a modified Benedict–Webb–Rubin type with 32 adjustable coefficients. Acceptable agreement of C_v predictions with measurements was found. Published $C_v(\rho, T)$ data suitable for direct comparison with this study do not exist. The uncertainty of the C_v values is estimated to be less than 2.0% for vapor and 0.5% for liquid. The uncertainty of the vapor pressures is 1 kPa, and that of the density measurements is 0.1%.

KEY WORDS: calorimeter; chlorotrifluoromethane; density; equation of state; heat capacity; isochoric; liquid; R13; vapor; vapor pressure.

[1] Physical and Chemical Properties Division, National Institute of Standards and Technology, Boulder, Colorado 80305, U.S.A.
[2] To whom correspondence should be addressed.
[3] Present address: Chemical Engineering and Petroleum Refining Department, Colorado School of Mines, Golden, Colorado 80401, U.S.A.

0195-928X/00/0900-1097$18.00/0

1. INTRODUCTION

The behavior of the (p, ρ, T) surface constitutes one of the most important and fundamental properties of pure fluids. Among the chief uses of (p, ρ, T) data is its incorporation into data bases for development and testing of predictive models for thermodynamic properties of fluids. Comprehensive (p, ρ, T) measurements on broad classes of fluids are needed for this purpose. Derived properties, including C_v, are useful to establish the behavior of higher-order derivatives.

The thermophysical properties of chlorotrifluoromethane (R13) have been reviewed by Altunin et al. [1] who have presented a comprehensive survey of the world's literature through 1985. Unfortunately, much of the published (p, ρ, T) data covers only a limited range of temperature, or worse, was conducted with samples of questionable purity. Representative sources of single-phase (p, ρ, T) data include Michels et al. [2] whose data extend from 273 to 423 K, Kubota et al. [3] from 298 to 348 K, Castro-Gomez et al. [4] from 230 to 400 K, Albright and Martin [5] from 216 to 403 K, Oguchi et al. [6] from 282 to 372 K. Each of the studies [2–6] was conducted on high purity samples and presents original, unsmoothed results. The pressure and temperature ranges of these data are shown in Fig. 1. Other sources not shown in Fig. 1 include Reidel [7] from 194 to

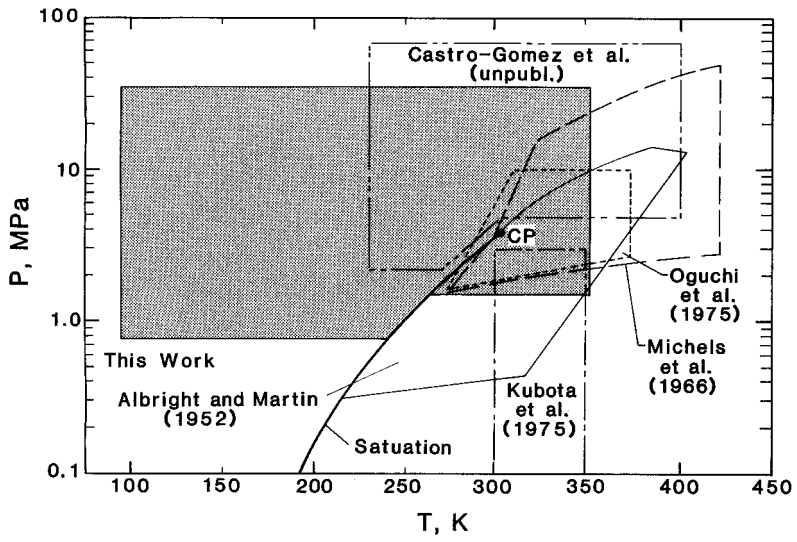

Fig. 1. Pressure–temperature regions of selected (p, ρ, T) studies of R13: this work Michels et al. [2]; Kubota et al. [3]; Castro-Gomez et al. [4]; Albright and Martin [5]; Oguchi et al. [6].

333 K (vapor densities), and Geller and Porichanskii [8] from 98 to 296 K. Altunin et al. [1] dismissed the (p, ρ, T) data of Ref. 7 due to possible impurities and insufficiently accurate pressure measurements (0.3 to 0.5%). Some doubt was cast on the data of Ref. 8 due to a lack of certain usual and customary corrections in their calculation formula [1]. Thus, from 92 to 216 K, no validated (p, ρ, T) data exist for liquid R13. Also, we found intercomparisons of density measurements to be hampered by the lack of one data set which overlaps all of the others. Thus, when this work began there existed a need for internally consistent (p, ρ, T) data covering temperatures from near the freezing line to supercritical conditions, over a broad range of densities ranging from dilute vapor to compressed liquid. Such data, we believe, would form the data base needed to model (p, ρ, T) relations of chlorotrifluoromethane with an equation of state.

Representative sources of vapor pressures include Fernandez-Fassnacht and Del Rio [9], Reidel [7], Rasskazov et al. [10], Oguchi et al. [11], Albright and Martin [5], and Jaeger [12]. There is poor consistency among these published data. At temperatures above 250 K, there appear to be two groupings of data separated by 0.2 to 0.3% in pressure [1]. Additional vapor pressure data at $T > 250$ K may resolve this discrepancy, and allow us to select the most reliable data for fitting an equation.

A literature search uncovered no published C_v data for R13. Measurements of molar heat capacity are necessary to develop a new equation of state which accurately predicts thermal properties.

2. MEASUREMENTS

2.1. (p, ρ, T) Apparatus

The apparatus used in this work has a long history including studies of pure fluids and mixtures [13, 14]. Since details of the apparatus are available in previous publications, they will be briefly reviewed here. The experimental method employed has been called the isochoric (constant volume) method and is used without change from widely known procedures. In this method, a sample of fixed mass is confined in a container of nearly fixed volume. The volume of the container is accurately known as a function of pressure and temperature. The temperature is changed in increments, and pressure is measured at each temperature until the upper limit of temperature or pressure (35 MPa) is attained. When the upper limit of the run has been reached, the sample is withdrawn into a weighing cylinder that is immersed in boiling liquid nitrogen. This gravimetric technique gives the sample mass from the difference of precise weighings

before and after the sample is trapped in the weighing cylinder. The density of the sample fluid is determined from a knowledge of the sample mass and the volume of the cell at each pressure and temperature on the run. The cells volume (28.787 ± 0.014 cm^3, 300 K) had been calibrated [14] by H_2 expansions under controlled conditions. Measured densities have an uncertainty of 0.1%.

Since the volume is only approximately constant, we will refer to a run as an isometric. Pressures are measured by reading the average period of vibration, over a given time interval, of an oscillating quartz crystal transducer which is connected to the sample container (cell) through a fine diameter (0.03 cm OD) capillary. The transducer, thermostatted at 333.15 ± 0.05 K, has been calibrated versus an oil-lubricated piston gauge, accurate to 0.01%. Calibrations performed before and after completion of this study show our transducer is extremely stable over a period of a year. We found stability to be better than 0.003% of the pressure. Measured pressures have an uncertainty of 0.03%. Temperatures are measured with a platinum resistance thermometer (PRT) circuit which incorporates a 25 ohm PRT calibrated on the IPTS-68 by NIST, a precision current source, a 10 ohm standard resistor calibrated by NIST, low thermal emf solder connections, ultralow thermal emf relays, and a 6 1/2 digit nanovoltmeter. Measured temperatures have an uncertainty of 0.03 K. The current source supplies the thermometry circuit with 2 mA and is equipped with relays capable of reversing the direction of current in the circuit. Thus, we are able to average forward and reverse readings of potential, completely eliminating errors associated with any spurious emf's. Readings of our transducer's period of oscillation and readings of potentials in the thermometry circuit are communicated to the host microcomputer by an IEEE-488 standard interface. In turn, relays and power supplies are controlled with digital and analog signals, respectively. A customized computer program is responsible for automated data aquisition, control, and data processing.

When charging a sample to the cell, the storage cylinder was inverted and raised above the cell. In this manner, liquid flowed freely into the cell. The cell temperature was adjusted according to an estimate provided by a preliminary equation of state developed during an earlier stage of this project, until the target density was obtained.

Vapor pressures were measured in the (p, ρ, T) apparatus using a static method. The cell was filled to one-half its volume with liquid R13. The cell was then cooled to its initial temperature and allowed to equilibrate at a fixed temperature before its pressure was recorded by the microcomputer. The temperature was then raised in steps until it reached 300 K.

2.2. C_v Apparatus

The heat capacity measurements in this study were performed in the calorimeter described by Goodwin [13] and Magee [15]. Briefly, in this method, a sample of well-known mass (or number of moles N) is confined to a bomb of approximately 73 cm^3 volume; the exact volume varies with temperature and pressure. When a precisely measured electrical energy (Q) is applied, the resulting temperature rise ($\Delta T = T_2 - T_1$) is measured. When the energy (Q_0) required to heat the empty bomb is subtracted from the total, the heat capacity is

$$C_v \cong \frac{(Q - Q_0)}{N \Delta T} \tag{1}$$

For this study, a sample was charged to the bomb, then the charge valve was sealed. The bomb and its contents were then cooled to a temperature just above the saturation point. Then, measurements were begun and continued in the single-phase region until either the upper temperature (300 K) or pressure (35 MPa) was attained. At the completion of a run, some of the sample was discharged to obtain the next filling density. A series of such runs at different mass densities (ρ) completes the $C_v(\rho, T)$ surface for the substance under study.

2.3. Sample

Our sample was analyzed by gas chromatography in two analytical laboratories and found to consist of 30 ppm dichlorodifluoromethane, 50 ppm bromotrifluoromethane, 392 ppm carbon tetrafluoride, and the balance was chlorotrifluoromethane. Accounting for the observed impurities, the purity was determined to be 0.9995 mole fraction.

3. RESULTS

3.1. Measurements

Table I reports the temperatures, pressures, and densities for 106 states on a total of 15 isometrics ranging from 1.0 to 18.0 $mol \cdot dm^{-3}$. The experimental temperatures range from 92 to 350 K, and pressures extend to 35 MPa. In Tables I to III, the temperatures are presented on ITS-90 after they were converted from IPTS-68 by using a table of adjustments [16]. Table II gives measurements of temperatures and vapor pressures from 250 to 302 K.

Table I. (p, ρ, T) Measurements and Calculated Densities for Chlorotrifluoromethane (R13)

T (K)	P (bar)	ρ_{exp} $(mol \cdot dm^{-3})$	ρ_{calc} $(mol \cdot dm^{-3})$	Diff.[a] (%)
289.996	28.357	2.0085	1.9996	0.443
299.994	30.945	2.0064	2.0011	0.264
309.991	33.439	2.0026	1.9992	0.168
319.988	35.892	2.0004	1.9990	0.070
329.985	38.265	1.9983	1.9960	0.113
339.983	40.598	1.9960	1.9932	0.140
349.980	42.892	1.9937	1.9904	0.166
319.988	35.885	2.0004	1.9984	0.104
299.994	35.918	3.0150	3.0210	−0.197
309.991	40.234	3.0114	3.0219	−0.346
319.988	44.391	3.0077	3.0125	−0.162
329.985	48.438	3.0036	3.0034	0.005
339.983	52.402	2.9992	2.9956	0.121
349.980	56.315	2.9943	2.9902	0.139
319.988	44.377	3.0077	3.0104	−0.090
309.991	43.529	4.0287	4.0863	−1.409
319.988	49.558	4.0230	4.0491	−0.644
329.985	55.460	4.0164	4.0271	−0.267
339.983	61.271	4.0089	4.0120	−0.077
349.980	67.007	4.0015	4.0004	0.026
319.988	49.555	4.0230	4.0483	−0.626
309.991	45.209	5.0151	5.0681	−1.046
319.988	53.127	5.0072	5.0364	−0.579
329.985	60.989	4.9977	5.0190	−0.424
339.983	68.810	4.9880	5.0067	−0.374
349.980	76.597	4.9800	4.9970	−0.340
319.988	53.120	5.0072	5.0342	−0.536
309.991	46.587	6.0112	5.9349	1.287
319.988	56.658	6.0007	5.9863	0.242
329.985	66.845	5.9882	6.0007	−0.208
339.983	77.051	5.9779	5.9995	−0.360
349.980	87.324	5.9699	5.9985	−0.476
319.988	56.640	6.0007	5.9820	0.313
309.991	49.038	7.0221	6.9543	0.975
319.988	61.987	7.0077	6.9905	0.247
329.985	75.197	6.9935	7.0032	−0.137

Table I. *(Continued)*

T (K)	P (bar)	ρ_{exp} (mol · dm^{-3})	ρ_{calc} (mol · dm^{-3})	Diff.[a] (%)
339.983	88.556	6.9836	7.0057	−0.315
349.980	102.040	6.9756	7.0059	−0.432
319.988	61.989	7.0077	6.9907	0.244
309.991	55.331	8.0227	8.0115	0.139
319.988	72.315	8.0039	8.0051	−0.015
329.985	89.620	7.9913	8.0001	−0.110
339.983	107.150	7.9819	7.9957	−0.172
349.980	124.829	7.9738	7.9919	−0.226
319.988	72.341	8.0038	8.0068	−0.037
299.994	49.037	9.0284	9.0266	0.020
309.991	71.229	9.0053	9.0073	−0.023
319.988	93.786	8.9902	8.9917	−0.016
329.985	116.665	8.9797	8.9808	−0.012
339.983	139.769	8.9707	8.9733	−0.029
349.980	162.953	8.9623	8.9671	−0.054
319.988	93.807	8.9902	8.9923	−0.023
289.996	48.481	10.0341	10.0315	0.026
299.994	77.721	10.0063	10.0068	−0.005
309.991	107.465	9.9911	9.9881	0.030
319.988	137.554	9.9802	9.9743	0.059
329.985	167.862	9.9705	9.9644	0.062
339.983	198.202	9.9614	9.9566	0.048
349.980	228.520	9.9526	9.9512	0.015
279.999	61.584	10.9960	10.9997	−0.034
289.996	99.823	10.9704	10.9728	−0.022
299.994	139.015	10.9571	10.9568	0.002
309.991	178.424	10.9461	10.9440	0.019
319.988	217.750	10.9360	10.9331	0.026
329.985	257.055	10.9263	10.9257	0.006
339.983	296.169	10.9169	10.9207	−0.035
260.003	57.082	12.0201	12.0221	−0.016
270.001	107.169	11.9884	11.9923	−0.033
279.999	159.065	11.9738	11.9769	−0.026
289.996	210.978	11.9619	11.9636	−0.014
299.994	262.762	11.9509	11.9533	−0.020
309.991	314.219	11.9404	11.9459	−0.046

Table I. *(Continued)*

T (K)	P (bar)	ρ_{exp} (mol · dm^{-3})	ρ_{calc} (mol · dm^{-3})	Diff.[a] (%)
235.008	40.800	13.0398	13.0349	0.037
240.007	72.553	13.0129	13.0129	−0.001
245.006	105.392	12.9975	12.9973	0.002
250.005	139.373	12.9881	12.9879	0.002
255.004	173.567	12.9805	12.9801	0.004
260.003	207.761	12.9737	12.9730	0.005
265.002	241.891	12.9673	12.9668	0.004
275.000	309.710	12.9553	12.9565	−0.009
279.999	343.370	12.9495	12.9526	−0.024
240.007	72.564	13.0129	13.0130	−0.001
210.010	46.491	14.0483	14.0477	0.004
215.010	86.780	14.0174	14.0178	−0.003
220.009	130.962	14.0039	14.0034	0.004
225.009	176.184	13.9947	13.9936	0.008
230.008	221.470	13.9868	13.9853	0.011
235.008	266.529	13.9796	13.9778	0.013
240.007	311.389	13.9728	13.9716	0.008
215.010	86.777	14.0174	14.0178	−0.003
200.011	7.724	14.2773	14.2761	0.008
205.011	52.911	14.2532	14.2538	−0.004
210.010	95.554	14.2237	14.2236	0.001
215.010	142.715	14.2113	14.2098	0.011
220.009	190.660	14.2022	14.1997	0.018
225.009	238.616	14.1944	14.1912	0.022
230.008	286.349	14.1871	14.1840	0.022
235.008	333.802	14.1802	14.1780	0.016
155.014	101.716	16.0172	16.0290	−0.073
160.014	180.116	16.0016	16.0065	−0.030
165.013	260.325	15.9907	15.9900	0.004
170.013	340.144	15.9813	15.9766	0.029
94.008	79.585	17.8951	17.8841	0.061
98.009	183.325	17.8720	17.8733	−0.007
100.009	240.192	17.8651	17.8684	−0.019
104.010	354.317	17.8534	17.8547	−0.007

[a] Diff. $= 100(\rho - \rho_{calc})/\rho_{calc}$.

Table II. Vapor Pressure Measurements for Chlorotrifluoromethane (R13)

T (K)	P_σ (MPa)
Sample 1	
260.00	1.3856
270.00	1.8132
280.00	2.3317
290.00	2.9543
299.99	3.7041
300.99	3.7887
301.99	3.8758
Sample 2	
250.00	1.0366
260.00	1.3862
270.00	1.8132
280.00	2.3315
290.00	2.9537
299.99	3.7049

Table III. Measurements of C_v and Calculated Values for Chlorotrifluoromethane (R13)

T (K)	ρ ($mol \cdot dm^{-3}$)	P (MPa)	ρ_{calc} ($mol \cdot dm^{-3}$)	Diff.[a] (%)	adj.[b]	C_v	$C_{v,calc}$[c]	Diff.[d] (%)
					($J \cdot mol^{-1} \cdot K^{-1}$)			
100.960	17.8201	21.4199	17.8098	0.06	7.20	52.270	52.365	−0.18
103.746	17.7882	28.3674	17.7923	−0.02	7.09	52.330	52.522	−0.37
99.814	17.8254	17.3976	17.8039	0.12	7.23	52.050	52.553	−0.96
102.614	17.7921	24.4295	17.7881	0.02	7.14	52.030	52.536	−0.96
105.392	17.7618	31.3106	17.7699	−0.04	7.06	52.280	52.766	−0.92
123.158	17.0302	11.3106	17.0189	0.06	5.41	51.590	54.115	−4.67
125.889	17.0098	16.8481	17.0025	0.04	5.48	51.440	53.715	−4.24
128.599	16.9915	22.3426	16.9866	0.03	5.50	51.600	53.567	−3.67
131.284	16.9746	27.7369	16.9711	0.02	5.53	51.860	53.627	−3.29
133.943	16.9585	33.0115	16.9560	0.02	5.53	52.230	53.848	−3.00
154.440	16.0295	9.2897	16.0316	−0.02	4.11	52.770	52.427	0.65
157.063	16.0182	13.3520	16.0185	0.00	4.21	52.640	52.478	0.31
159.673	16.0080	17.4125	16.0064	0.01	4.28	52.690	52.659	0.06
162.261	15.9980	21.4140	15.9950	0.02	4.34	52.970	52.943	0.05
164.828	15.9880	25.3508	15.9840	0.02	4.39	53.230	53.311	−0.15
167.381	15.9778	29.2134	15.9733	0.03	4.45	53.750	53.746	0.01
184.170	15.0935	9.7132	15.0927	0.01	3.33	54.640	53.878	1.41
186.712	15.0862	12.7917	15.0841	0.07	3.39	54.560	54.117	0.82

Table III. *(Continued)*

T (K)	ρ (mol · dm^{-3})	P (MPa)	ρ_{calc} (mol · dm^{-3})	Diff.[a] (%)	adj.[b]	C_v	$C_{v,calc}$[c]	Diff.[d] (%)
					(J · mol^{-1} · K^{-1})			
189.242	15.0790	15.8498	15.0759	0.02	3.44	54.680	54.413	0.49
191.753	15.0717	18.8716	15.0680	0.03	3.50	54.960	54.769	0.35
196.739	15.0561	24.7970	15.0526	0.02	3.59	55.640	55.607	0.06
199.206	15.0481	27.6972	15.0453	0.02	3.63	56.020	56.073	−0.09
201.657	15.0398	30.5561	15.0383	0.01	3.67	56.240	56.563	−0.57
204.096	15.0311	33.3654	15.0313	0.00	3.71	56.890	57.068	−0.31
216.249	13.9990	9.3008	13.9966	0.02	2.53	57.360	57.351	0.02
219.056	13.9929	11.8263	13.9906	0.02	2.59	57.650	57.605	0.08
221.843	13.9872	14.3382	13.9849	0.01	2.63	57.750	57.910	−0.28
224.618	13.9809	16.8246	13.9791	0.01	2.67	57.970	58.259	−0.50
227.372	13.9745	19.2824	13.9734	0.01	2.72	58.460	58.644	−0.31
230.120	13.9676	21.7125	13.9674	0.00	2.76	58.960	59.059	−0.17
232.845	13.9607	24.1186	13.9618	−0.01	2.79	59.090	59.497	−0.68
235.559	13.9534	26.4959	13.9563	−0.02	2.83	59.330	59.954	−1.04
238.265	13.9458	28.8521	13.9509	−0.04	2.86	59.610	60.430	−1.36
240.958	13.9380	31.1783	13.9456	−0.05	2.89	60.080	60.916	−1.37
263.658	12.0291	7.7243	12.0273	0.01	1.46	62.420	63.386	−1.52
266.792	12.0257	9.3693	12.0235	0.02	1.50	62.630	63.492	−1.36
269.923	12.0222	11.0144	12.0194	0.02	1.53	62.640	63.648	−1.58
273.035	12.0186	12.6522	12.0154	0.03	1.55	62.900	63.845	−1.48
276.138	12.0144	14.2779	12.0107	0.03	1.58	63.570	64.079	−0.79
279.232	12.0098	15.8954	12.0060	0.03	1.61	63.870	64.344	−0.74
282.300	12.0057	17.5051	12.0019	0.03	1.63	63.600	64.635	−1.60
285.355	12.0010	19.1007	11.9975	0.03	1.66	64.100	64.948	−1.31
288.410	11.9956	20.6837	11.9927	0.03	1.69	65.000	65.282	−0.43
291.444	11.9908	22.2629	11.9888	0.02	1.70	64.710	65.632	−1.40
294.472	11.9854	23.8293	11.9846	0.00	1.73	65.090	65.996	−1.37
297.494	11.9799	25.3866	11.9805	0.00	1.75	65.430	66.372	−1.42
300.508	11.9742	26.9345	11.9767	−0.02	1.77	65.790	66.758	−1.45
291.954	10.0177	5.3960	10.0211	−0.03	0.79	67.720	67.887	−0.25
295.184	10.0137	6.3459	10.0152	−0.01	0.82	67.280	67.751	−0.69
298.415	10.0116	7.3080	10.0110	0.01	0.84	67.290	67.662	−0.55
301.645	10.0103	8.2775	10.0075	0.02	0.86	67.330	67.621	−0.43
304.876	10.0088	9.2507	10.0040	0.05	0.87	67.380	67.623	−0.36
308.099	10.0074	10.2256	10.0006	0.06	0.89	66.990	67.665	−1.00
311.317	10.0059	11.2014	9.9972	0.09	0.91	67.050	67.741	−1.02
314.540	10.0040	12.1792	9.9937	0.10	0.92	67.050	67.850	−1.18
317.767	10.0016	13.1583	9.9900	0.12	0.94	67.270	67.989	−1.06
320.993	9.9995	14.1400	9.9867	0.12	0.95	67.280	68.153	−1.28
324.231	9.9968	15.1237	9.9832	0.14	0.97	67.860	68.341	−0.70
327.479	9.9941	16.1118	9.9800	0.14	0.98	68.030	68.551	−0.76
330.738	9.9916	17.1051	9.9772	0.15	1.00	67.980	68.780	−1.16
334.017	9.9887	18.1027	9.9744	0.15	1.01	68.290	69.027	−1.07
337.321	9.9859	19.1086	9.9718	0.14	1.03	68.110	69.292	−1.71

Table III. *(Continued)*

T (K)	ρ (mol · dm^{-3})	P (MPa)	ρ_{calc} (mol · dm^{-3})	Diff.[a] (%)	adj.[b]	C_v	$C_{v,calc}$[c]	Diff.[d] (%)
					(J · mol^{-1} · K^{-1})			
303.705	8.1210	4.5480	8.1079	0.16	0.47	72.500	71.926	0.80
307.164	8.1190	5.1411	8.1092	0.12	0.48	71.970	71.513	0.64
310.633	8.1150	5.7430	8.1105	0.06	0.50	71.630	71.171	0.64
314.122	8.1112	6.3549	8.1122	−0.02	0.51	70.940	70.888	0.07
324.635	8.1046	8.2324	8.1177	−0.16	0.55	70.490	70.346	0.20
328.155	8.1028	8.8683	8.1182	−0.19	0.56	70.030	70.257	−0.32
331.675	8.1020	9.5085	8.1191	−0.21	0.57	69.810	70.207	−0.57
335.214	8.1009	10.1536	8.1193	−0.23	0.58	69.810	70.193	−0.55
311.757	5.9310	4.8201	5.8841	0.80	0.32	79.030	75.115	5.21
315.505	5.9688	5.2002	5.9353	0.57	0.33	77.120	74.491	3.53
319.285	5.9837	5.5853	5.9643	0.33	0.34	75.580	73.964	2.18
326.881	5.9939	6.3646	5.9957	−0.03	0.35	73.690	73.133	0.76
330.723	5.9969	6.7621	6.0065	−0.16	0.36	73.040	72.808	0.32
334.592	5.9966	7.1621	6.0126	−0.26	0.37	72.250	72.538	−0.40
338.472	5.9971	7.5650	6.0180	−0.35	0.37	72.010	72.319	−0.43
312.614	4.1234	4.5381	4.1769	−1.29	0.27	78.310	74.571	5.01
316.673	4.1351	4.7955	4.1764	−0.99	0.27	76.750	74.042	3.66
320.748	4.1429	5.0520	4.1742	−0.75	0.27	75.240	73.576	2.26
324.840	4.1481	5.3076	4.1712	−0.56	0.27	74.670	73.169	2.05
328.958	4.1508	5.5630	4.1675	−0.40	0.27	73.680	72.819	1.18
333.098	4.1530	5.8187	4.1648	−0.28	0.28	72.750	72.522	0.31
337.263	4.1546	6.0747	4.1621	−0.17	0.28	72.190	72.277	−0.12
297.421	2.0767	3.0769	2.0709	0.29	0.19	69.350	69.290	0.09
302.057	2.0769	3.2022	2.0734	0.17	0.19	69.430	68.986	0.64
306.702	2.0770	3.3256	2.0746	0.12	0.19	69.250	68.746	0.73
311.351	2.0772	3.4474	2.0752	0.09	0.19	68.820	68.564	0.37
316.004	2.0774	3.5680	2.0755	0.07	0.19	68.920	68.435	0.71
320.667	2.0775	3.6874	2.0755	0.12	0.20	69.340	68.357	1.44
325.339	2.0776	3.8061	2.0756	0.12	0.20	68.960	68.318	0.94
274.044	1.0457	1.7494	1.0405	0.53	0.15	63.020	63.601	−0.91
279.076	1.0452	1.8087	1.0413	0.36	0.15	62.800	63.538	−1.16
284.093	1.0449	1.8669	1.0418	0.31	0.15	63.830	63.538	0.46
289.112	1.0448	1.9245	1.0423	0.26	0.15	63.460	63.587	−0.20
294.120	1.0450	1.9815	1.0428	0.21	0.15	63.030	63.679	−1.02
299.121	1.0451	2.0378	1.0432	0.17	0.15	63.580	63.809	−0.36
314.135	1.0456	2.2044	1.0444	0.16	0.15	63.460	64.388	−1.44
319.139	1.0458	2.2594	1.0448	0.11	0.16	64.540	64.630	−0.14
324.156	1.0460	2.3140	1.0452	0.08	0.16	63.760	64.893	−1.75
329.189	1.0462	2.3687	1.0456	0.04	0.16	65.130	65.174	−0.07

[a] Diff. $= 100(\rho - \rho_{calc})/\rho_{calc}$.
[b] Equation (2).
[c] Equation (3).
[d] Diff. $= 100(C_v - C_{v,calc})/C_{v,calc}$.

For the heat capacities, significant adjustments must be applied to the raw data for the energy required to heat the empty calorimeter from the initial (T_1) to the final temperature (T_2). This is accomplished using the results of previous experiments done with a thoroughly evacuated bomb. These results were fitted to a 12-parameter polynomial $Q_0(T)$ given by Magee [15]. Additionally, an adjustment for PV work done by the fluid on the thin-walled bomb as the pressure rises from P_1 to P_2 is applied for each point. Corrections for PV work on the bomb are given by

$$C_{PV} = k[\, T_2(\partial P/\partial T)_{\rho_2} - \Delta P/2\,]\, \Delta V_m/\Delta T \tag{2}$$

where $k = 1000\ \mathrm{J \cdot MPa^{-1} \cdot dm^{-3}}$, the pressure rise is $\Delta P = P_2 - P_1$, and the volume change per mole is $\Delta v_m = \rho_2^{-1} - \rho_1^{-1}$. The derivative has been calculated with an equation of state discussed in a later section.

Table III gives the raw data and final values of the single-phase gaseous or liquid heat capacity. Data for a total of 101 state conditions are given. A correction for PV work on the bomb, given by Eq. (2), has been applied. Given under the column headed by Adj.[a], the magnitude of this adjustment ranges from 0.2 to 14% of the final heat capacity values. The final experimental C_v values are plotted in Fig. 2. The calculated C_v values

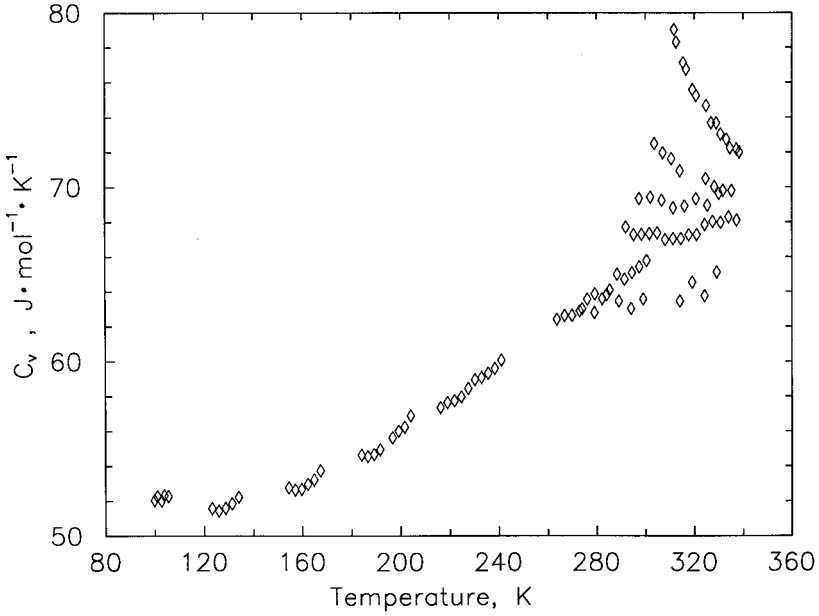

Fig. 2. Molar heat capacity at constant volume C_v measurements for R13: ◇, this work.

in Table III were derived from the equation of state discussed later with values of the heat capacity for the ideal gas [C_v^0] using the relation,

$$C_v(T, \rho) = C_v^0(T) - T \int_0^\rho (\partial^2 P/\partial T^2)_\rho \, d\rho/\rho^2 \tag{3}$$

The deviations of the experimental values from those calculated in this way are plotted in Fig. 3. This figure shows that the predicted values are generally within $\pm 2\%$ of the measurements,with the following exceptions: at densities around 6 mol · dm^{-3} and at temperatures less than 20 K above T_c, where the calculated C_v is too small by as much as 5% due to the close proximity of the critical point; and, at $\rho = 17$ mol · dm^{-3} at temperatures between 123 and 134 K, where the calculated C_v is too large by as much as 5%. Overall, the root-mean-square deviation of experimental values of C_v is 1.52%.

3.2. Analysis of Uncertainties

For the (p, ρ, T) apparatus, the uncertainty in temperature is 0.03 K, and in pressure it is 0.01% at $p > 3$ MPa and 0.05% at $p < 3$ MPa. The

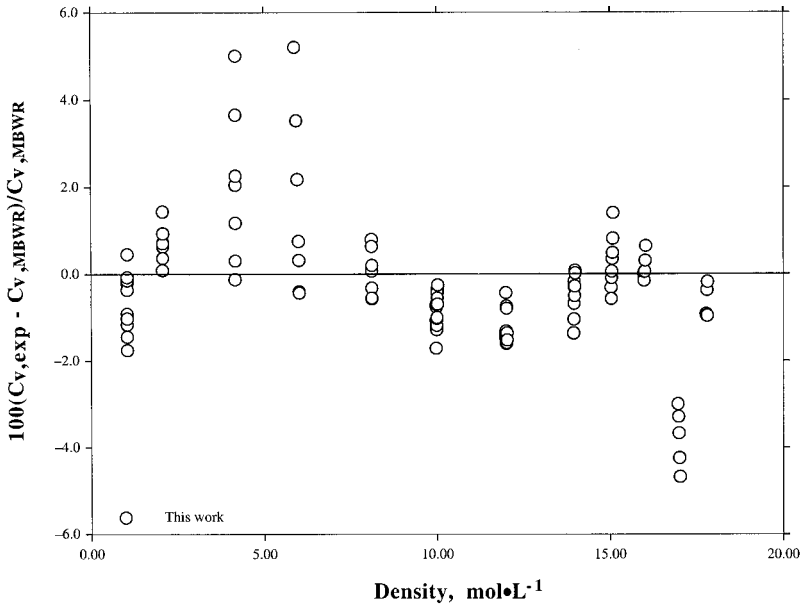

Fig. 3. Deviations of values of C_v from the equation of state: ○, this work.

uncertainty in density depends on the propagated uncertainty in both T and p, as well as from the volume calibrations (0.02%), and the mass measurement (0.01%). Overall the uncertainty of the measured density is 0.1%.

The uncertainty in C_v values arises from several sources. Primarily, the uncertainty of this method is limited by how accurately we can measure the temperature rise. The platinum resistance thermometer has been calibrated on the IPTS-68 by NIST, leading to an uncertainty of 0.002 K due to the calibration. Other factors, including gradients on the bomb, radiation to the exposed head of the thermometer, and time-dependendent drift of the ice point resistance lead to an overall uncertainty of $\sigma_t = 0.03$ K for the absolute temperature measurement. Uncertainty estimates of the relative temperature, however, are calculated differently. The temperatures assigned to the beginning (T_1) and to the end (T_2) of a heating interval are determined by extrapolation of a linear drift (approximately $-0.0005\ \mathrm{K \cdot min^{-1}}$) to the midpoint time of the interval. This procedure leads to an uncertainty of 0.002 K for T_1 and T_2, and consequently 0.004 K for the temperature rise, $\Delta T = T_2 - T_1$. For a typical experimental value of ΔT of 4 K, this corresponds to an uncertainty of 0.1%. The energy applied to the calorimeter is the integral of the product of the applied potential and current from the initial to the final heating time; its uncertainty is 0.01%. The energy applied to the empty calorimeter has been measured in repeated experiments and fit to a function of temperature [15]; its uncertainty is 0.02%. The moles of substance was determined within 0.02%. A correction for PV work on the bomb leads to an additional 0.02% uncertainty. For pressure, the uncertainty due to the piston gauge calibration is added to the cross term $[(\sigma_t)(\mathrm{d}P/\mathrm{d}T)_\varrho]$ to yield an overall maximum probable uncertainty which varies from 0.02 to 1.0%, increasing steadily with the slope of the (p, ρ, T) isochore to the maximum at the highest density and lowest pressure of the study. However, the pressure uncertainty does not appreciably contribute to the overall uncertainty for molar heat capacity. Combining the various sources of experimental uncertainty, we arrive at an estimated uncertainty of 2.0% for vapor-phase and 0.5% for liquid-phase C_v values.

4. TEST EQUATION OF STATE FOR R13

4.1. Fitting Procedure

In order to conveniently analyze the new measurement results and to compare them with published results, a test equation of state formulation was developed. The modified Benedict–Webb–Rubin [17] equation of state

(MBWR) was chosen to represent the (p, ρ, T) surface of R13 because of its ability to represent a wide range of fluid-phase behavior. This form of the BWR equation of state used to describe R13 behavior has 32 coefficients, and also has a fixed critical temperature, critical density, and critical pressure. The form of the equation is given below. The critical values and the coeffcients are given in Table IV. The equation was constrained to the two critical point conditions,

$$(\partial P/\partial V)_{T_c} = 0, \qquad (\partial^2 P/\partial V^2)_{T_c} = 0 \tag{4}$$

The pressure at the critical density and temperature was also constrained in developing the correlation, so that

$$P(\rho_c, T_c) = P_c \tag{5}$$

For the overall MBWR fit, several types of data were used in the correlation. In total, 249 (p, ρ, T) results from this study, from Kubota et al. [3], and from Albright and Martin [5] were the primary data used in the least-squares fit of the surface. Second virial data from Refs. 2, 18, and 19 were also used in the MBWR fit. The functional form of the MBWR equation of state is in terms of pressure, and is given by,

$$P = \rho RT + \sum_{n=2}^{9} a_n \rho^n + \exp(-\delta^2) \sum_{n=10}^{15} a_n \rho^{2n-17} \tag{6}$$

where $\delta = \rho/\rho_c$, ρ_c is the critical density, and the temperature dependence of the a_n are polynomials in terms of T^{-1} described in Ref. 17. Density deviations for the selected data are shown in Fig. 4.

The saturation boundary should be adequately described by the equation of state; to ensure a close fit in the two-phase region, we used 54 evenly-spaced saturation points between 90 and 302 K, which were generated by the ancillary equations for the saturation boundary. The two-phase points generated in this manner were given fairly low emphasis in the overall weighting scheme, but this data enabled us to help the equation of state closely describe the saturation boundary conditions.

The highest data-type weight was on the heat capacity data, while the vapor pressure, saturated liquid density and the (p, ρ, T) data recieved the second highest overall weighting. Second virial coefficients were assigned a weight factor which was 50% of the (p, ρ, T) data. Due to the poor precision of the available measured vapor density data, the ancillary saturated vapor density equation derived from the inconsistent data was given a very low weight in the fitting of the MBWR.

Table IV. Coefficients of the Equation of State

I	a_n
1	$0.427710490378 \times 10^{-2}$
2	$0.106603397093 \times 10^{1}$
3	$-0.383065097813 \times 10^{2}$
4	$0.661580211522 \times 10^{4}$
5	$-0.800160780370 \times 10^{6}$
6	$-0.406405755462 \times 10^{-2}$
7	$0.561380767634 \times 10^{1}$
8	$-0.247694806929 \times 10^{4}$
9	$-0.639834580892 \times 10^{5}$
10	$0.198818486764 \times 10^{-3}$
11	-0.206916891385
12	$0.749317872337 \times 10^{2}$
13	$-0.431471653965 \times 10^{-2}$
14	$0.181741326553 \times 10^{1}$
15	$-0.206066849491 \times 10^{2}$
16	-0.136681208829
17	$0.260496240940 \times 10^{-2}$
18	0.287244312242
19	$-0.105459756169 \times 10^{-1}$
20	$0.582404815872 \times 10^{6}$
21	$-0.455721947029 \times 10^{8}$
22	$0.114174177352 \times 10^{5}$
23	$0.265590236008 \times 10^{6}$
24	$0.135249873550 \times 10^{3}$
25	$0.128289104267 \times 10^{4}$
26	0.800900540368
27	$-0.703307137789 \times 10^{4}$
28	$0.235567665577 \times 10^{-2}$
29	$0.131830636112 \times 10^{1}$
30	$-0.115187941781 \times 10^{-4}$
31	$0.564530387616 \times 10^{-2}$
32	0.336242130107

$T_c = 302.0$ K
$P_c = 38.79$ bar
$\rho_c = 5.58$ mol · dm^{-3}
$R = 0.0831434$ bar · dm^{-3} · mol^{-1} · K^{-1}
Molar mass = 104.459 kg · kg-mol^{-1}

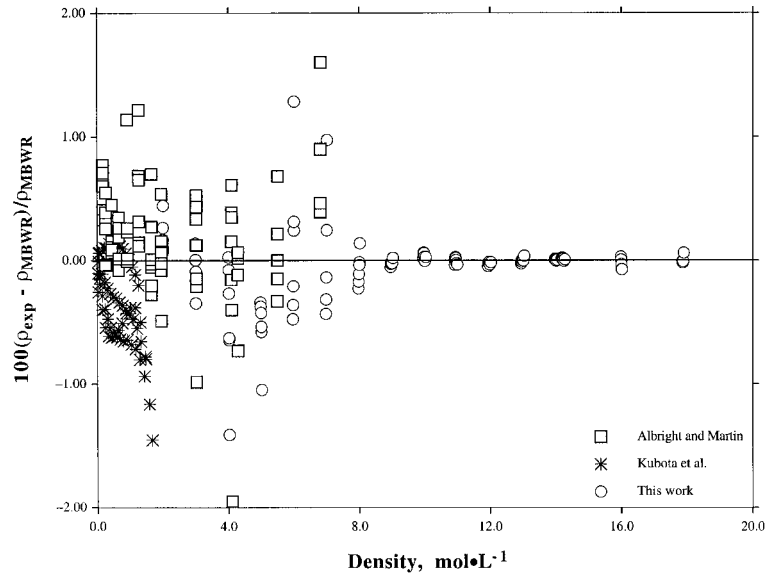

Fig. 4. Deviations of measured densities from the equation of state: ○, this work; ∗, Kubota et al. [3]; □, Albright and Martin [5].

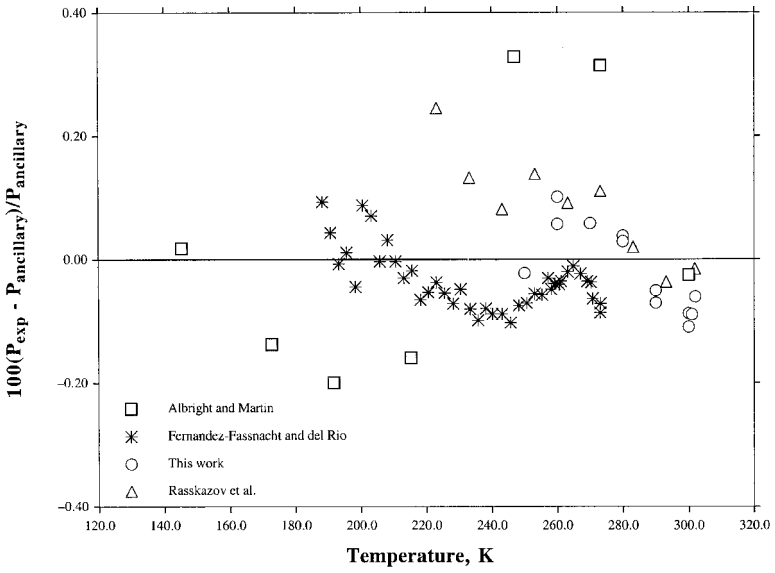

Fig. 5. Deviations of vapor pressures from the $P_\sigma(T)$ equation: ○, this work; □, Albright and Martin [5]; ∗, Fernandez-Fassnacht and del Rio [9]; △, Rasskazov et al. [10].

4.2. Liquid-Vapor Saturation Boundary

The saturation properties can be calculated from the MBWR, by a Maxwell construction technique in the two-phase region, but it is much more useful to have separate correlations for the saturation properties. For ease in calculating the saturation properties, we present separate correlations for the saturation vapor pressure P_σ, the saturated liquid density ρ_{sl}, and the saturated vapor density ρ_{sv}. These correlations have the same critical values as the final MBWR equation of state, and were used as input data in the development of the equation of state, as discussed below.

4.3. Ancillary Equations for the Two-Phase Boundary

The ancillary equations Eqs. (7) to (9) for the saturated vapor pressure and the liquid and vapor densities for the two-phase region were developed with the critical constants given in Table IV. These ancillary equation critical values are identical to those used in the final MBWR correlation for the entire (p, ρ, T) surface, and are within the accepted limits for the experimentally determined critical point. The published critical temperature (IPTS-68) for R13 has ranged from 301.880 K [11] to 302.29 K [2]. The corresponding critical pressure has ranged from 3.879 MPa [11] to 3.911 MPa [2] and the critical density has varied from 5.53 $\text{mol} \cdot \text{dm}^{-3}$ [20] to 5.58 $\text{mol} \cdot \text{dm}^{-3}$ [11]. The ancillary critical parameters were chosen after several other values were used in the saturation boundary fits, as these particular critical values resulted in the overall best-fit of the equation of state. The value of $\beta = 0.35$ was fixed. Several equations were tested for the vapor pressure correlation before the most descriptive equation was selected. Many parameters were tried for the liquid and vapor density equations; the present values were superior to any others that were tested.

The various ancillary equation coefficients were obtained by the method of least squares, with weights varying by author, temperature, and density to obtain the closest approximation to the chosen data. Outliers in each of the two-phase property data sets were excluded from the fits if they did not appear to be reasonably consistent with other data from their particular source, or if the entire data set appeared to have some type of systematic measurement error.

4.4. Saturated Liquid Density

The saturation liquid density for R13 was fitted with the expression,

$$\rho_{sl} = \rho_c[1 + g_1\varepsilon^{\beta} + g_2\varepsilon^{2/3} + g_3\varepsilon + g_4\varepsilon^{4/3}] \tag{7}$$

Table V. Coefficients of the Saturated Liquid Density ρ_{sl} Equation[a, b]

Coeff.	Value
g_1	1.72714665
g_2	1.08253980
g_3	−1.18452379
g_4	1.05523638
$T_c = 302.0$ K	
$\rho_c = 582.88122$ kg · m^{-3}	
$\beta = 0.35$	

[a] Density in kg · m^{-3}.
[b] T range: 130 to 301 K.

where $\varepsilon = 1 - T/T_c$. The data of Albright and Martin [5], Reidel [7], Oguchi et al. [11] and Geller and Porichanskii [21] were used in the fit of Eq. (7). The coefficients of Eq. (7) are found in Table V. Deviations of the experimental data from Eq. (7) are shown in Fig. 6.

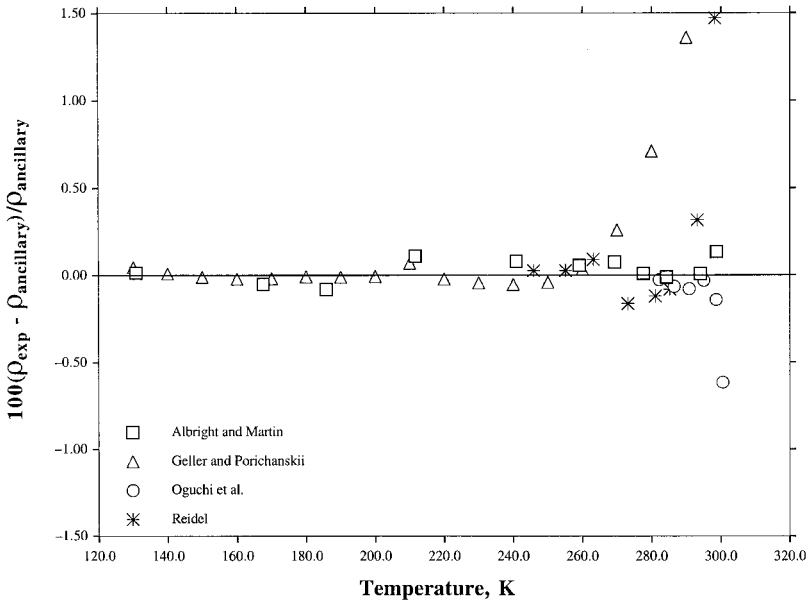

Fig. 6. Deviations of saturated liquid densities from the $\rho_{sl}(T)$ equation: □, Albright and Martin [5]; ○, Oguchi et al. [6]; ∗, Reidel [7]; △, Geller and Porichanskii [8].

4.5. Saturated Vapor Pressure

The functional form of the saturated vapor pressure ancillary equation was chosen for its flexibilty and accuracy in fitting various vapor-pressure data. The data from Albright and Martin [5], Fernandez-Fassnacht and del Rio [9], Rasskazov et al. [10], and this work were used in the least-squares fit to obtain the four coefficients in the equation, which are given in Table VI. The equation has the form given below,

$$P_\sigma = P_c e^{(a_1\varepsilon + a_2\varepsilon^{3/2} + a_3\varepsilon^3 + a_4\varepsilon^6)/(1-\varepsilon)} \tag{8}$$

where $\varepsilon = 1 - T/T_c$ and P_c is the critical pressure. The critical values were constrained to the same values used in the saturated liquid density correlation. An equation with seven coefficients was also tried, but we deemed the four-term equation to be sufficiently accurate for our purposes, since the data do not have the accuracy needed to justify a seven-term form. At temperatures above 250 K, the measurements in Table II helped to resolve the discrepancy between previously published measurements which revealed two separate curves separated by up to 0.4%. In this case, our results agree closely with the lower-pressure curve of Fernandez-Fassnacht and del Rio [9], as shown in Fig. 7. As a result, we dropped the Reidel [7] data from consideration in the fitting process. There is only one source of reliable P_σ data for R13 below 188 K, and below 145 K, there are none.

4.6. Saturated Vapor Density

In selecting an equation for the saturated vapor density of a compound, two conditions should be adequately described by the equation. The low-density, ideal gas behavior should be predicted by the functional form, and

Table VI. Coefficients of the Vapor Pressure Equation[a, b]

Coeff.	Value
a_1	−6.83254667
a_2	1.34035019
a_3	−2.24839837
a_4	−2.09814527
$T_c = 302.0$ K	
$P_c = 3879$ kPa	

[a] Pressure in kPa.
[b] T range: 188 to 301 K.

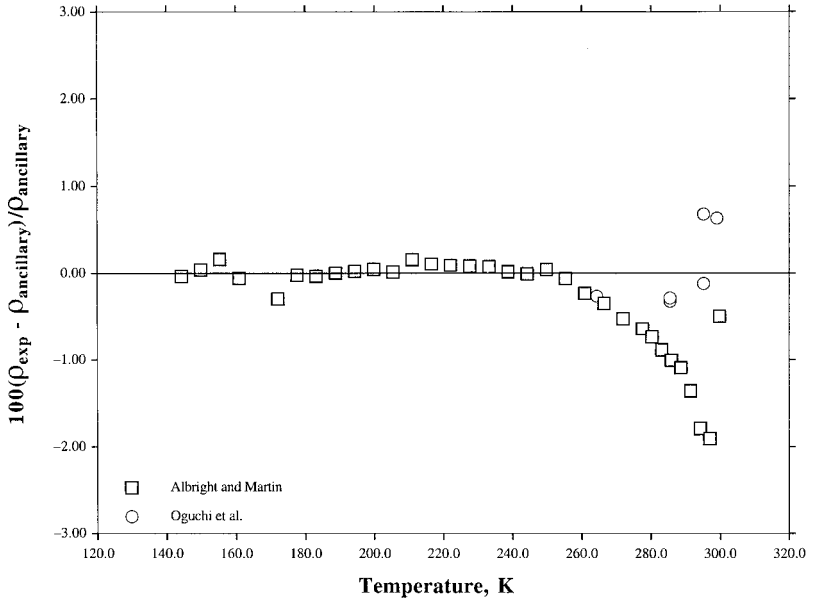

Fig. 7. Deviations of saturated vapor densities from the $\rho_{sv}(T)$ equation: □, Albright and Martin [5]; ○, Oguchi et al. [6].

the nonideal behavior near the critical point should also be described by the equation [22]. The final equation used to correlate R13 is given below. The equation describes the behavior of the fluid over the entire density range, although the available vapor density data are not very consistent, and thus, the accuracy of much of the data is questionable.

$$\frac{(Z-1)[T/T_c]^8}{[P_\sigma/P_c](Z_c-1)} - 1 = [b_0\varepsilon^\beta + b_1\varepsilon^{2\beta} + b_2\varepsilon + b_3\varepsilon^2 + b_4\varepsilon^4]/[1 + b_5\varepsilon] \tag{9}$$

where Z_c is the compressibility factor at the critical point and P_σ is the vapor pressure derived from Eq. (8). The value of β is 0.35, and the critical values are the same as those used in the other ancillary equations. The coefficients are given in Table VII. The experimental data of Albright and Martin [5] and Oguchi et al. [6] were used in the final saturated vapor density correlation. Deviations of these data from Eq. (9) are shown in Fig. 7. The coefficients obtained by least-squares give a maximum error of 0.7 percent for the points used in the analysis.

Table VII. Coefficients of the Saturated Vapor Density ρ_{sv} Equation[a, b]

Coeff.	Value
b_0	−0.661217962
b_1	−1.57673859
b_2	−1.18952113
b_3	1.48087202
b_4	−0.769130869
b_5	1.62181160
$T_c = 302.0$ K	
$P_c = 3879$ kPa	
$\rho_c = 582.88122$ kg · m^{-3}	
$\beta = 0.35$	

[a] Density in kg · m^{-3}.
[b] T range: 144 to 300K.

4.7. Ideal Gas Heat Capacities

The functional form of the ideal gas heat capacity ancillary equation was chosen for its flexibilty and simplicity. The data of Albright and Martin [5] and Chen et al. [23] were used in the least-squares fit to obtain the four coefficients in the equation, which are given in Table VIII. The equation has the form

$$C_p^0/R = a_0 + a_1 T_r + a_2 T_r^2 + a_3 T_r^3 \tag{10}$$

where $R = 8.314471$ J · mol^{-1} · K^{-1}, $T_r = T/T_c$ and $T_c = 302.00$ K is the critical temperature. Deviations of ideal-gas heat capacities from Eq. (10) are shown in Fig. 8.

Table VIII. Coefficients of the Ideal-Gas Heat Capacity C_p^0 Equation[a]

Coeff.	Value
c_1	1.86012334
c_2	8.07314520
c_3	−1.87713639
c_4	$3.17242858 \times 10^{-2}$

[a] T range: 50 to 500 K.

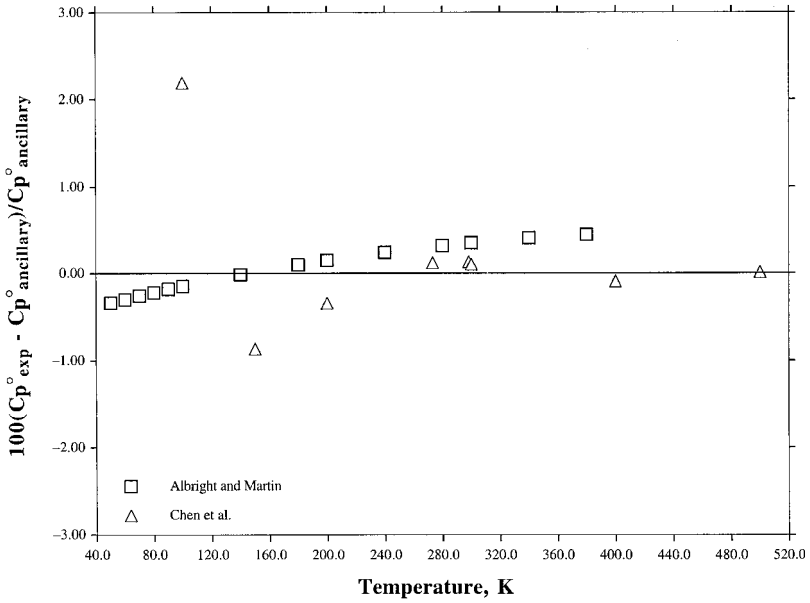

Fig. 8. Deviations of ideal gas heat capacities from the $C_p^0(T)$ equation: □, Albright and Martin [5]; △, Chen et al. [23].

4.8. Comparison of Calculated and Experimental Properties

The primary R13 data are those that were used in determining the best-fit correlations. Other available experimental data were not used in obtaining the correlations, for various reasons, such as lack of internal precision, unknown experimental methods, poor accuracy, and disagreement with more reliable data. A representative discussion is given below, rather than an exhaustive analysis, as the various published data are more thoroughly discussed by their original authors.

For all deviation plots, the convention used is that the zero line represents the appropriate derived correlation, from Eqs. (7) to (9) and the associated tables. The percentage deviations for each experimental point are calculated as 100(exp − calc)/calc where exp represents the experimental value of a property and calc is the value computed from the correlation.

Figure 4 shows that there is good agreement among the density measurements of Albright and Martin [3], Kubota et al. [5], and this work. The root-mean-square (RMS) deviation for the data of Albright and Martin is 0.46%, for Kubota et al. it is 0.34%, and for this work it is 0.29%.

In Fig. 5, we show the deviations of the primary experimental vapor pressure data from the correlation of Eq. (8). The agreement of Eq. (8)

with the selected data of Refs. 5, 7, 9, and 11 and with this work is rather good, with an overall RMS deviation of 0.09%. In total, 67 points were used for the vapor pressure equation in the temperature range from 145 to 302 K; the correlation should only be used within these temperature limits, as this is the region within which the calculational error does not exceed $\pm 0.33\%$ for the primary data.

Figures 6 and 7 give a detailed view of the fits to the selected saturated density data that were used in the fit. We expect Eq. (7) to give saturated liquid densities with an uncertainty of 0.2% from 130 to 298 K. Similarly, we expect Eq. (9) to give saturated vapor densities with an uncertainty of 0.7% from 144 to 299 K.

Figure 8 shows the deviations of experimental ideal-gas heat capacities from the correlation, Eq. (10). Systematic differences with published data are less than 1%, with the exception of one datum at 100 K, which differs by +2% from both Eq. (10) and the data of Albright and Martin.

The range of applicability of the MBWR is approximately from 94 to 403 K at pressures up to 35 MPa. We expect this equation to give densities with an approximate uncertainty of 0.15%, except in the critical region or near the saturation curve at temperatures below 130 K. We have found that the equation will predict heat capacity at constant volume with an uncertainty of approximately 2%, except in the critical region and at temperatures below 130 K. Because of its rather obvious deficiencies, we do not recommend its general use for calculation of thermodynamic properties of R13. However, it is useful tool for intercomparison of measurements. Improvement would be realized from new measurements of vapor pressure, saturated-liquid density, and saturated-liquid heat capacity in regions where data are needed.

ACKNOWLEDGMENTS

The authors are grateful to Brian Tripp for valuable technical assistance. We thank E. I. DuPont de Nemours and Co. for providing the sample.

NOMENCLATURE

C_v	Molar heat capacity at constant volume
C_v^0	Molar heat capacity in the ideal gas state
V_{bomb}	Volume of the calorimeter containing sample
P	Pressure
ΔP	Pressure rise during a heating interval
P_σ	Vapor pressure

T	Temperature
T_1, T_2	Temperature at start and end of heating interval
ΔT	Temperature rise during a heating interval
T_r	Reduced temperature, T/T_c
ε	Reduced temperature deviation from critical, $1 - T/T_c$
Q	Calorimetric heat energy input to bomb and sample
Q_0	Calorimetric heat energy input to empty bomb
N	Moles of substance in the calorimeter
ρ	Fluid density
ρ_r	Reduced density, ρ/ρ_c

REFERENCES

1. V. V. Altunin, V. Z. Geller, E. A. Kremenevskaya, I. I. Perelshtein, and E. K. Petrov, *Thermophsical Properties of Freons Methane Series Part 2*. English-language ed., T. B. Selover, Jr., ed. (Hemisphere, Washington, DC, 1987).
2. A. Michels, T. Wassenaar, G. J. Wolkers, C. Prins, and L. Klundert, *J. Chem. Eng. Data* **11**:449 (1966).
3. H. Kubota, Y. Tanaka, and T. Makita, *Rev. Phys. Chem. Japan* 538 (1975).
4. R. C. Castro-Gomez, G. A. Iglesias-Silva, W. R. Lau, J. C. Holste, K. N. Marsh, K. R. Hall, and P. T. Eubank, personal communication (Texas A&M University, College Station, 1986).
5. L. F. Albright and J. J. Martin, *Ind. Eng. Chem.* **44**:188 (1952).
6. K. Oguchi, I. Tanishita, K. Watanabe, T. Yamaguchi, and A. Sasayama, *Bull. JSME* **18**:1448 (1975).
7. L. Reidel, *Ztschr. ges. Kälte-Ind.* **48**:9 (1941).
8. V. Z. Geller and E. G. Porichanskii, *Kholodilnaya Tekhn. Tekhnol.* **29**:43 (1979).
9. E. Fernandez-Fassnacht and F. del Rio, *Cryogenics* **25**:204 (1985).
10. D. S. Rasskazov, E. K. Petrov, and E. R. Ushmaikin, *Teplofiz. Svoistva Veshchestv Material.* **14**:7 (1980).
11. K. Oguchi, I. Tanishita, K. Watanabe, T. Yamaguchi, and A. Sasayama, *Bull. JSME* **18**:1456 (1975).
12. H. P. Jaeger, *Die Kälte* **7**:276 (1973).
13. R. D. Goodwin, *J. Res. Natl. Bur. Stand. (US) C* **65**:231 (1961).
14. J. W. Magee and J. F. Ely, *Int. J. Thermophys.* **9**:547 (1988).
15. J. W. Magee, *J. Res. Natl. Inst. Stand. Tech.* **96**:725 (1991).
16. H. Preston-Thomas, *Metrologia* **27**:3 (1990).
17. R. T Jacobsen and R. B. Stewart, *J. Phys. Chem. Ref. Data* **2**:757 (1973).
18. R. G. Kunz and R. S. Kapner, *J. Chem. Eng. Data* **14**:190 (1969).
19. B. Schramm and R. Gehrmann, Unpublished data communicated to J. H. Dymond and E. B. Smith, *The Virial Coefficients of Pure Gases and Mixtures* (Clarendon Press, Oxford, 1980).
20. W. Rathjen and J. Straub, *Wärme-und Stoffübertragung* **14**:59 (1980).
21. V. Z. Geller and E. G. Porichanskii, *Kholodilnaya Tekn.* **2**:42 (1980).
22. R. D. Goodwin and W. M. Haynes, *Natl. Bur. Stand. (U.S.) Monograph 170* (U.S. GPO, Washington, DC, 1982).
23. S. S. Chen, R. C. Wilhoit, and B. J. Zwolinski, *J. Phys. Chem. Ref. Data* **5**:571 (1976).